Available online www.jocpr.com

Journal of Chemical and Pharmaceutical Research, 2017, 9(6):281-289

Research Article

ISSN : 0975-7384
CODEN(USA) : JCPRC5

Synthesis and Characterization of Boron and 2-Aminophenol Schiff Base Ligands with Their Cu(II) and Pt(IV) Complexes and Evaluation as Antimicrobial Agents

Asmaa Mohammed Noori Khaleel* and Marwa Issa Jaafar

University of Baghdad, College of Science, Chemistry Department, Baghdad, Iraq

---

ABSTRACT

Synthesis, Characterization and biological study of two Schiff base ligands derived from 2-aminophenol and 4-bromoacetophenone (1:1) (L_1) and boron Schiff base which was derived from L_1 and sodium borohydride (1:1) (L_2). Cu (II) and Pt (IV) complexes of the Schiff base ligands were synthesized. The prepared compounds have been investigated by molar conductivity, elemental analysis, FTIR, ^{1}H ^{13} CNMR, thermal analysis, UV-VIS, as well as atomic absorption and magnetic susceptibility. The biological study of the ligands and their metal complexes were carried out against E-coli, Staphylococcus, as bacteria species, Candida and Mycrosporium Canis as fungi.

Keywords: Schiff base; 2-aminophenol

INTRODUCTION

The Schiff bases have a wide range of uses and applications because these compounds have excellent properties such as structural similarities with biological molecules, simple preparation methods with flexibility [1], biological activity as antiviral, antileukemic, antibacterial, enzymatic reaction inhibitors and biocidal which is essential for plant growth regulators [2]. Boron compounds have been well known since ancient times where used to prepare hard glasses and glazes. Today the uses of boron compounds expended to include semiconductors, hard materials and antitumor medicine [3-5]. Boron is an electron deficient which possess four valance orbitals and only three electrons, boron tendency to fill the vacant orbital and this promote the electron acceptor behavior and lead to increase the stability of imine group (C=N) of boron Schiff base, therefore the organoborane compounds are more stable than organometallic compounds [6]. Boron Schiff bases have many applications such as catalyst [7], determination of enantiopurity of chiral amino alcohols [8], photoelectronic application [6,9] and nutraceutical industry [10]. In this paper we report the synthesis, structural characterization and biological evaluation of two Schiff base ligands, 2-aminophenol Schiff base (L_1) and boron Schiff base (L_2) with their Cu (II) and Pt (IV) complexes.

EXPERIMENTAL SECTION

Material and Instruments

All chemicals used were of analytical reagent grade. Melting points were determined by using Gallenkamp melting point apparatus. Thermal analysis (TG and DTG) were performed by using METTLER TA4000 SYSTEM for L_1 and METTLER TOLEDO for L_2. The spectra of ^{1}H and ^{13}C NMR were recorded on (Bruker NMR spectrometer 400 MHz Avance III 400). The electronic spectra of all prepared compounds were recorded on (SHIMADZU 1800-UV spectrophotometer) in DMSO. FTIR were carried out in the range (400-4000) cm^{-1} using KBr disk for the ligands and CsI disk in the range (250-4000) cm^{-1} for metal complexes by using SHIMADZU 8400s spectrophotometer. Elemental microanalysis was carried out by (CHNS Elemental Analyzer CHNS-932). Metal contents were determined by using (Nov AA 350 spectrophotometer). Magnetic

susceptibility measurements were performed at room temperature by using (Auto Magnetic Susceptibility Balance Model Sherwood Scientific). Molar conductivity was measured in DMSO at room temperature by using Hunts Capacitor Trade Mark British made. Chloride contents were determined by using Mohr method.

Methods

Synthesis of 2-((1-(4-bromophenyl)ethylidine)amino)phenol (L_1):

This ligand has been prepared in our previous work [11].

Synthesis of 2-borane((1-(4-bromophenyl)ethylidene)amino)phenol (L_2):

A hot solution of Schiff base (L_1) (0.173 gm, 0.59 mmol) in 60 ml tetrahydrofurane (THF) was added gradually to a boiled suspension of sodium borohydride (0.045 gm, 1.19 mmol) in 10 ml THF. The mixture was heated under reflux for 16 hr with stirring and the color of solution changed from green to brown. The brown product was obtained by concentrated the reaction mixture and then a little amount of n-hexane was added, washed several times with n-hexane and dried in air (Figure 1).

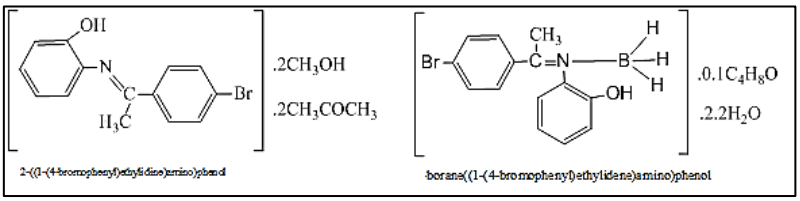

(L_1) (L_2)

Figure 1: The structures of synthesized ligands L_1 and L_2

Synthesis of Cu (II) complexes C_1 and C_3:

To a hot solution of L_1 (0.1 gm, 0.2128 mmol) in a mixture of methanol:aceton (2:1) was added a methanolic solution of $CuCl_2.2H_2O$ (0.0181 gm, 0.1064 mmol) for C_1 complex. The mixture was heated under reflux for four hours. Dark brown precipitate was obtained after evaporating part of the solvent and adding ether. Washed several times with ether and dried. The preparation method of copper complex (C_3) was similar to that of (C_1), using L_2 (0.0713 gm, 0.2034 mmol) with $CuCl_2.2H_2O$ (0.0173 gm, 0.1017 mmol).

Synthesis of platinum complexes C_2 and C_4:

The preparation methods of platinum complexes were similar to that of (C_1), using L_1 or L_2 0.1g (0.2128 and 0.2852 mmol) respectively and K_2PtCl_6 (0.0517g, 0.1064 mmol) in 6 ml DMSO for C_2 and (0.0693 g, 0.1426 mmol) in 24 ml DMSO for C_4 respectively.

RESULTS AND DISCUSSION

The physical and analytical data (Table 1) are agreement with suggested structures of studied compounds.

Table 1: The physical properties and analytical data for two ligands and their metal complexes

Symbol	Color	Yield%	m.p °C	CHN analysis Found(calc.)			M% vFound(calc.)	Cl% Found(calc.)
				C%	H%	N%		
L_1	Golden-brown	21.9	134-137	56.27	5.95	4.34	_	_
				-56.18	-6.8	-3		
L_2	Brown	57.2	>240	48.3	5.04	4.93	_	_
				-49.29	-5.8	-4		
C_1	Dark brown	48.3	>360	52.53	3.57	3.82	10.88	2.6
				-51.92	-3.7	-4.3	-9.87	-2.7
C_2	Dark brown	39.2	>360	24.42	2.55	1.59	_	2.8
				-23.43	-3.1	-2		-4.5
C_3	Dark brown	93.7	>360	32.7	4.09	1.89	4.82	7.4
				-33.79	-4.9	-2.8	-5.63	-7.1
C_4	Dark brown	92.9	>360	21	3.19	1.79	_	_
				-21.92	-4.2	-1.8		

IR Spectra

The data of IR spectra of studied ligands and their metal complexes are listed in Table 2 and the spectra of L_1 and L_2 are shown in Figure 2. The peaks appeared at (3420-3452) cm^{-1} were attributed to lattice water while the coordinated water was exhibited peaks at observed at (3379, 651) and (3406, 756) cm^{-1} [12-14]. The spectra of L_1, L_2, C_1 and C_2 were exhibited strong peaks at (3400-3520) cm^{-1} which were assigned to stretching vibration of OH group, this band was shifted to lower frequency in the spectrum of C_2 complex at 3400 cm^{-1} as a result of complexation [15,16] and disappeared in spectra of C_3 and C_4 because of the binding of metal ions with oxygen

atom of OH group. The band appeared at 2340 cm^{-1} in spectra of L_2, C_3 and C_4 assigned to vibrational mode of B-H [12]. The band at 1415 cm^{-1} in spectrum of L_2 was attributed to the stretching vibration of B-N, this band not changed in spectra of C_3 and C_4 complexes [12]. The azomethine group (C=N) exhibited peak at 1581 cm^{-1} for L_1 while this peak shifted to lower frequency at 1562 cm^{-1} for L_2 and this due to binding of BH_3 with nitrogen atom of C=N. The spectrum of metal complex C_2 showed shifted to lower frequency in this peak at 1577 cm^{-1} comparison with L_1 and the spectrum of C_1 exhibited change in profile of C=N peak, this due to the binding between N atom and metal ions [16,17]. Peaks that noticed at range 304-491 cm^{-1} were assigned to stretching vibration of M-Cl, M-O and M-N [13,15,18].

Table 2: IR spectra of two ligands and their metal complexes

Compound	υO-H	υB-H	υB-N	υC=N	H2O lattice (coordinate)	υM-O	υM-N	υM-Cl
L1	3448	-	-	1581	-	-	-	-
C1	3440	-	-	1583	-	-	387	312
C2	3400	-	-	1577	3420	500	435	318
L2	3520	2340	1415	1562	3425	-	-	-
C3	-	2340	1413	1566	3452	441	-	304
					-34,06,756			
C4	-	2340	1415	1565	3448	491	-	329
					-33,79,651			

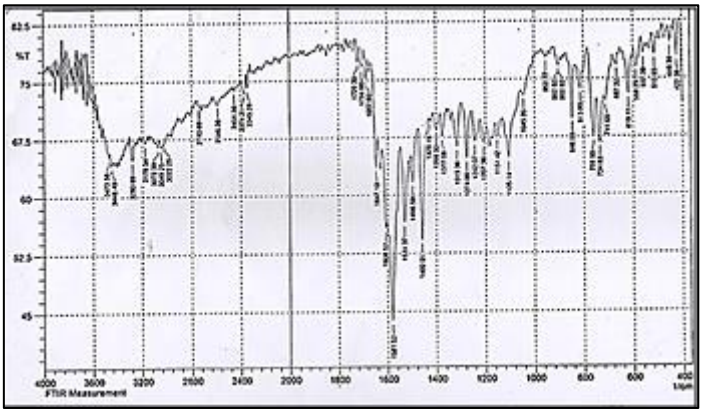

L_1

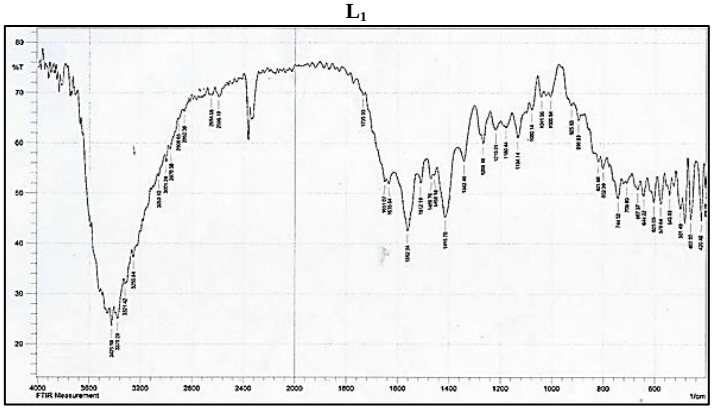

L_2

Figure 2: The IR spectra of ligands L1 and L2

^{1}HNMR Spectra

The data of ^{1}HNMR are listed in Table 3 and the NMR spectra in DMSO of L_1 and L_2 are shown in (Figure 3). The spectra of two ligands showed chemical shift at 8.9 and 8.5 ppm for L_1 and L_2 respectively and this due to OH proton [14]. The multiple peaks observed at the range δ(6.3-6.8) ppm referred to aromatic protons [19]. The spectrum of L_1 exhibited a peak at δ (1.9 ppm) which assigned to CH_3 protons and acetone (CH_3) [14,16]. Chemical shifts of methanolic CH_3 protons and the dissolved water in DMSO appeared at δ (3.3 ppm) [16]. The weak band appeared at δ (4.3 ppm) is due to methanolic OH proton [16]. The spectrum of L_2 exhibited peak at δ (1 ppm) which was referred to CH_3 protons [14,16]. The peak observed at (δ 1.65 ppm) attributed to THF protons (mark: 16), while the broad peak appeared at δ (3.4 ppm) due to protons of THF (mark: 17), BH, H_2O and dissolved water in DMSO [12-20]. Strong peak appeared at δ (2.5 ppm) was assigned to residual DMSO [12,14].

Table 3: Chemical shifts for 1HNMR of L1 and L2

L_1			L_2		
Chemical shifts δ(ppm)	**Mark**	**Assignments in DMSO**	**Chemical shifts δ(ppm)**	**Mark**	**Assignments in DMSO**
1.9,9H,s	8,16,18	CH_3 protons and CH_3 in acetone protons	1,3H,s	8	CH_3 protons
3.3,3H,s	15	Methanolic CH_3 protons and dissolved water in DMSO	1.65,4H,s	16	$2(CH_2)$ of THF
4.3,1H,s	15	Methanolic OH proton	3.4,9H,s	15,17,18	$BH,H_2O,2(CH_2)$ of THF and dissolved water in DMSO
6.3-6.6,8H,m	03-Jun	Aromatic protons	6.3-6.8,8H,m	03-Jun	Aromatic protons
	10,11,13,14			10,11,13,14	
8.9,1H,s	2	O-H proton	8.5,1H,s	2	O-H proton

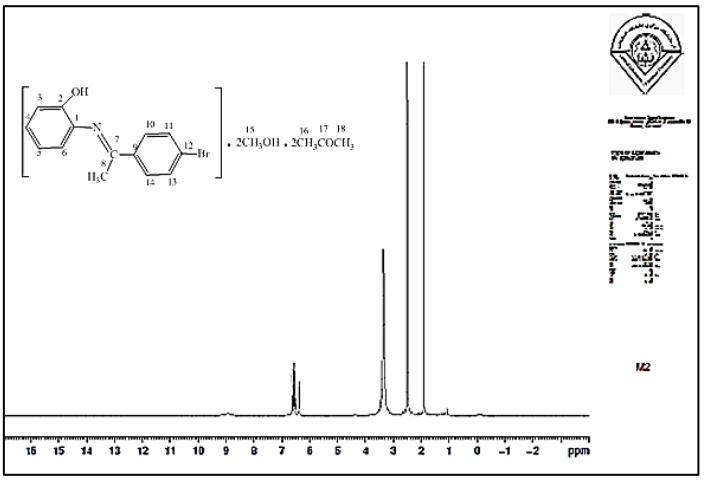

L_1

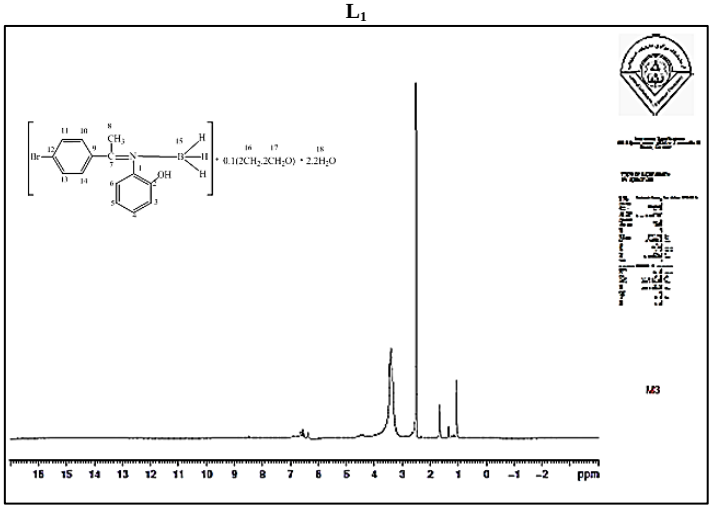

L_2

Figure 3: 1HNMR spectra of L_1 and L_2

^{13}CNMR Spectra

The data of ^{13}CNMR are listed in Table 4. The ligands spectra in DMSO exhibited multiple peaks at range δ(114-125.2) ppm which due to aromatic carbon [14]. The single peaks observed at δ(130.4, 125 ppm) for L_1 and L_2 respectively attributed to chemical shift of C-N (mark:1) [21]. The peak at δ (132.6 and 132.5 ppm) for L_1 and L_2 respectively due to carbon of C-Br [16]. Chemical shift of phenolic carbon (mark: 2) appeared at δ (144 and 144.1 ppm) for L_1 and L_2 respectively [16]. The azomethine carbon showed chemical shift at δ (172 and 166.1 ppm) for L_1 and L_2 respectively [14]. The spectrum of L_1 exhibited peak at δ (20 ppm) which due to CH_3 carbon [14], while the peak at δ (34 ppm) was attributed to CH_3 of acetone [16]. The methanolic carbon exhibited chemical shift at δ (49 ppm) and the carbon of acetone (mark: 17) showed chemical shift at δ (204 ppm) [16]. The spectrum of L_2 showed another peaks, the peak appeared at δ (18 ppm) which assigned to methyl group carbon [14]. The carbons of THF (mark: 16) showed a peak at δ (24.5 ppm), while the carbons

(mark:17) exhibited peak at δ(68.3 ppm) [16]. The peak appeared at δ(40 ppm) was attributed to chemical shift of DMSO [16].

Thermal Analysis TG and DTG

TG and DTG data of studied ligands are listed in Table 5 and their thermograms are showed in (Figure 4). The first step for each ligand involved loss of solvents and water molecules because of their low boiling points at temperature range (33.7-172.3°C) and (20.6-85°C) for L_1 and L_2 respectively. The thermogram of L_1 showed the decomposition of L_1 through four steps at temperature range (33.7-601.3°C) without residue, while the decomposition of L_2 carried out through four steps at temperature range (20.6-650°C) with residue and this means the L_2 is more stable than L_1 [22-24].

Table 4: Chemical shifts (ppm) for 13CNMR of L_1 and L_2

L_1			L_2		
Chemical shifts δ(ppm)	**Mark**	**Assignment inDMSO**	**Chemical shifts δ(ppm)**	**Mark**	**Assignment in DMSO**
20	8	Carbon of methyl group	18	8	Carbon of methyl group
34	16,18	Carbon of acetone	24.5	16	2(CH_2) of THF
49	15	Methanolic carbon	68.3	17	2(CH_2) of THF
114-125.2	03-Jun	Aromatic carbons	114.5-120.5	03-Jun	Aromatic carbon
	9,10,11,13,14			9,10,11,13,14	
130.4	1	Carbon of amine	125	1	Carbon of amine
132.6	12	Carbon of brom	132.5	12	Carbon of brom
144	2	Phenolic carbon	144.1	2	Phenolic carbon
172	7	Carbon of azomethine	166.1	7	Carbon of azomethine
204	17	Carbon of acetone			

Table 5: Thermal decomposition of L_1 and L_2

Compound	**Steps**	**Temp. range of Decomposition °C**	**Peak temp at DTG °C**	**% weight loss Found (calc.)**
L_1 C6H12NOBr.2CH3OH.2CH3COCH3 M.wt= 469.9	2 CH_3OH	33.7-172.3	146.3	
	2 CH_3COCH_3			38.83 (40.00)
	8 H			
	$C_6Br + C_6$	172.3-280.7	207	46.48 (47.64)
	C	280.7-354.3	324	3.17 (2.55)
	$CH_3 + N + OH$	354.3-601.3	458.3	11.53 (9.78)
L2 C14H15NOBBr.0.1C4H8O.2.2H2O M.wt= 350.52	0.1C_4H_4O	20.6-85	88	12.30(13.35)
	2.2H_2O			
	Br	85-170	178	21.53(22.79)
	BH_3+CH_3+OH	170-320	323	13.73(13.07)
	C_6H_4	320-446	480	22.13(21.68)
	C_6H_4CN(residue)	446-650	-	30.30(29.09)

Electronic Spectra, Magnetic Moments and Molar Conductivity

The data of UV-Vis spectra of L_1, L_2 and their metal complexes in DMSO are listed in Table 6. The spectra of ligands (Figure 5) showed the intense band at 40650 and 41493 cm^{-1} for L_1 and L_2 respectively due to $\pi \rightarrow \pi^*$ transition and weak intensity band at 23980 and 19758 cm^{-1} of L_1 and L_2 respectively which referred to $n \rightarrow \pi^*$ transition. The copper and platinum complexes of L_1 and L_2 exhibited blue shift of ligand bands ($\pi \rightarrow \pi^*$). The spectrum of copper complex (C_1) (Figure 5) showed three bands at 15329, 19794 and 20976 cm^{-1} which were assigned to $^2B_1g \rightarrow {}^2A_1g$, $^2B_1g \rightarrow {}^2B_2g$ and $^2B_1g \rightarrow {}^2Eg$ transitions respectively of tetragonally distorted octahedral Cu(II) complexes [14]. A three absorption bands were observed in the spectrum of copper complex (C_3) at 11030, 15480 and 19671 cm^{-1} which attributed to $^2B_1g \rightarrow {}^2A_1g$, $^2B_1g \rightarrow {}^2B_2g$ and $^2B_1g \rightarrow {}^2Eg$ transitions respectively, as well as the absorption band at 24154 cm^{-1} which were belong to charge transfer transition (C.T) [13,14,25].

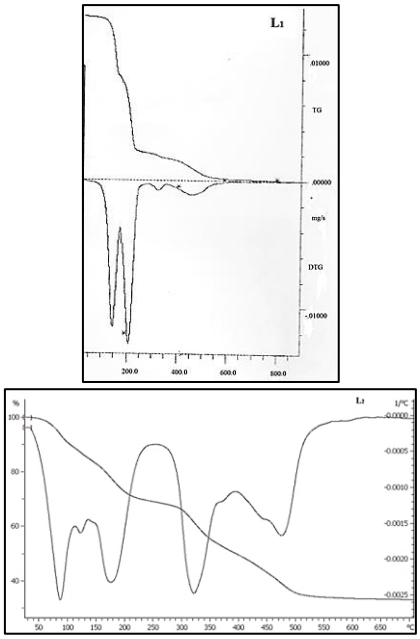

Figure 4: Thermograms of Ligands L_1 and L_2

The magnetic moments of copper complexes C_1 and C_3 were μ_{eff} =2.4 and 2.6 B.M of C_1 and C_2 respectively, these values due to octahedral geometry [26]. The spectrum of diamagnetic platinum complex C_2 showed bands at 12195, 22935 and 29614 cm^{-1} which assigned to $^1A_1g \rightarrow {}^3T_1g$ (H), $^1A_1g \rightarrow {}^3T_2g$ and $^1A_1g \rightarrow {}^1T_1g$(C.T) transition respectively of octahedral platinum (IV) complexes [13,27,28]. Two absorption bands were observed in spectrum of Pt(IV) complex (C_4) (Figure 5) at 11035 and 21643 cm^{-1} which were referred to $^1A_1g \rightarrow {}^3T_1g$(H) and $^1A_1g \rightarrow {}^3T_2g$ transitions respectively of octahedral platinum (IV) complexes. [13,27,28]. The molar conductivity data in DMSO were 0.033, 0.059, 0.121 and 0.163 $S.mol^{-1}.cm^{-1}$ for C_1, C_2, C_3 and C_4 complexes respectively indicating the nonelectrolytic properties of complexes [29]. The suggested structures of complexes were shown in (Figure 6).

Biological Screening

The data of biological activity were listed in Table 7. The studied compounds and starting materials were tested as antibacterial and antifungal agents against gram negative bacteria (*E. coli*), gram positive bacteria *(Staphylococcus aureus*), (*Candida*) and *(Mycrosporium Canis*). The test was carried out by diffusion method for studied compounds in DMSO and concentration 10^{-2} M. The tested compounds exhibited different activities against *Staphylococcus aureus*, *Candida* and *Mycrosporium canis*, while these compounds were inactive against *E. coli*. The results have been compared with three kinds of antibiotics cephalexim, cefatoxim and ketoconazole.

Table 6: Electronic spectra, magnetic moment and molar conductance with suggested structures of L_1 and L_2 complexes

Symbol	Band position cm-1	Assignments	$\mu_{eff.\ B.M}$	Molar Conductivity $S.mol^{-1}.cm^{-1}$	Suggested structures
$C_{1\ Cu(II)}$	υ_1 15329	$^2B_1g \rightarrow {}^2A_1g$	2.4	0.0337	octahedral
	υ_2 19794	$^2B_1g \rightarrow {}^2B_2g$			
	υ_3 20976	$^2B_1g \rightarrow {}^2Eg$(C.T)			
$C_{2\ Pt(IV)}$	υ_1 12195	$^1A_1g \rightarrow {}^3T_1g$(H)	diamagnetic	0.0591	octahedral
	υ_2 22935	$^1A_1g \rightarrow {}^3T_2g$			
	υ_3 29614	$^1A_1g \rightarrow {}^1T_1g$(C.T)			
$C_{3\ Cu(II)}$	υ_1 11030	$^2B_1g \rightarrow {}^2A_1g$	2.6	0.121	octahedral
	υ_2 15480	$^2B_1g \rightarrow {}^2B_2g$			
	υ_3 19671	$^2B_1g \rightarrow {}^2Eg$			
	υ_4 24154	L→M(C.T)			
$C_{4\ Pt(IV)}$	υ_1 11035	$^1A_1g \rightarrow {}^3T_1g$(H)	diamagnetic	0.163	octahedral
	υ_2 21643	$^1A_1g \rightarrow {}^3T_2g$			

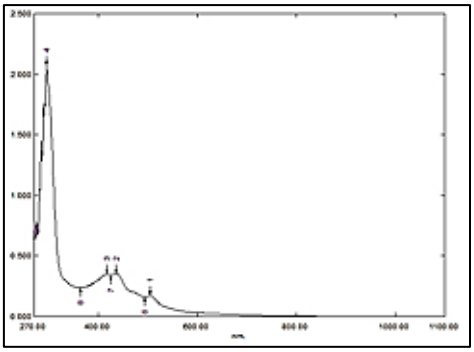

L_1

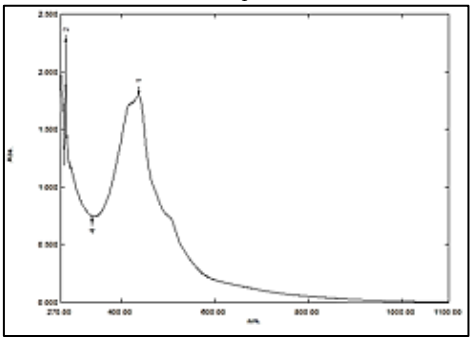

C_1

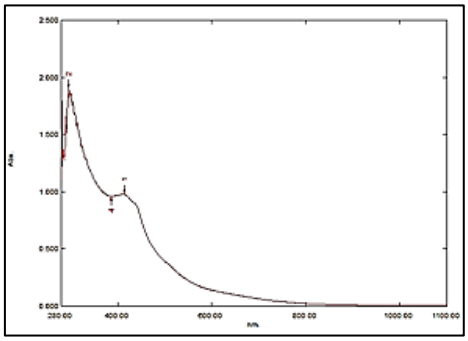

L_2

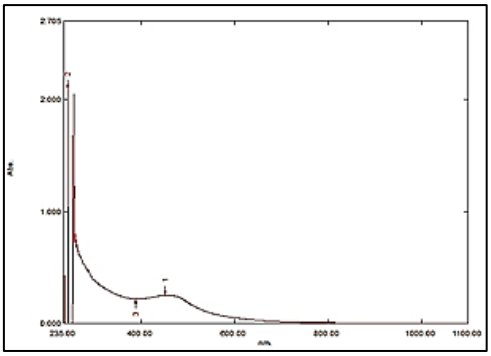

C_4

Figure 5: UV-VIS spectra of L_1, L_2, C_1 and C_4 complexes

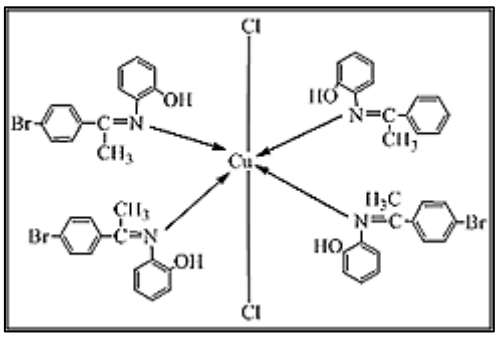

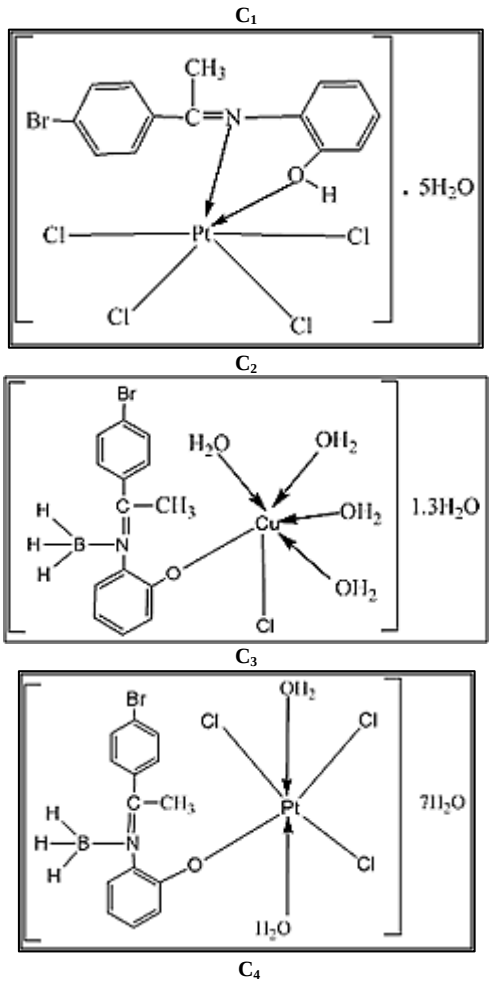

Figure 6: The suggested structures of synthesized complexes

Table 7: Antibacterial and antifungal activity of two ligands and their metal complexes

Compounds	***Staphylococcus aureus* diameter mm**	***E. coli* diameter mm**	**Candida diameter mm**	***Mycrosporium Canis* diameter mm**
DMSO	zero	zero	zero	zero
2-aminophenol	36	zero	18	zero
4-bromoacetophenone	zero	zero	zero	zero
Sodium borohydride	zero	zero	zero	zero
L_1	20	zero	12	15
L_2	23	zero	12	zero
C_1	32	zero	34	23
C_2	20	zero	10	zero
C_3	20	zero	15	13
C_4	zero	zero	zero	zero
Cephalexim	25	zero	-	-
Cefatoxim	48	45	-	-
Ketoconazole	-	-	zero	20

REFERENCES

[1] AMX John; MR Arockia; JM Margaret; *J Chem Pharm Res*. **2012**, 4, 669-672.
[2] BK Rai; K Rachana; T Amrita; Hakur. *Orient J Chem*. **2012**, 28, 943-948.
[3] N Anastassia; IB Alexander; Z Hua-jin; W Lai-sheng. *Coordin Chem Rev*. **2006**, 250, 2811-2866.
[4] A Abdullatif. *Int J Eng Adv Tech*. **2015**, 4, 147-155.
[5] SM Douglas; JS Kenneth. *Nucle Instrumen Met Phy Res A*. **2004**, 517, 180-188.
[6] H Qiufei; Z Liyan; Z Hongyu; W Yue; J Shimei. *Springer*. **2007**, 126, 447-451.
[7] M Amitabha; JD Lauren; ES Jeffrey; PP Bijal; P Sean; AA David. *Inorg Chem*. **2006**, 45, 9213-9224.
[8] MK Andrew. Ph.D Thesis, University of Bath, **2008**.
[9] ACN Rodrego; Ph.D Thesis, University of Autonoma Denuevoleon, **2014**.
[10] B Anca-Mihael; B Andrei; B Florentina; P Alina; N Johny; EB Ludovic; B Cornelia; DM George. *Rev Chim*. **2014**, 65, 84-86.
[11] MNK Asmaa; IJ Marwa. *IOSR J Appl Chem*. **2016**, 9, 4-144.
[12] MNK Asmaa. *Iraqi J Sci*. **2015**, 56, 2762-2772.
[13] JA Ahlam; MNK Asmaa. *Bioinorg Chem Appl*. **2009**, 1-12.
[14] JA Ahlam; MNK Asmaa. *Bioinorg Chem Appl*. **2013**, 1-14.
[15] AS Kabeer; S Khaled. *Canadian J Trans*. **2015**, 3, 207-224.
[16] MS Robert. 6th Edition, John wiley and Sons Ink, Newyork, **1997**.
[17] A Xavier; N Srividhya. *IOSR J Appl Chem*. **2014**, 7, 6-15.
[18] MM Ritika; VD Barhat. *Int J Chem Tech Res*. **2014**, 6, 1003-1012.
[19] NK Chaudhary. *Arch Appl Sci Res*. **2013**, 5, 227-231.
[20] GR Fulmer; AJM Miller; NH Sherden; HE Gottlieb; A Nudelman; BM Stoltz; JE Bercaw; KI Goldberg. *Organometallics*. **2010**, 29, 2176-2179.
[21] K Ismet; A Aysel. *Chinese J Polymer Sci*. **2009**, 27, 465-477.
[22] GR Pandhare; VM Shinde; YH Deshpande. *Rasayan J Chem*. **2008**, 1, 337-341.
[23] O Sahin; AN Bulutcu. *Turk J Chem*. **2003**, 27, 197-207.
[24] A Magda; R Pode; C Muntean; M Medeleanu; A Popa. *J Serb Chem Soc*. **2010**, 75, 951-963.
[25] ABP Lever. Elsevier Publishing Co. Amsterdam-London, New York. **1968**.
[26] GM Gehad; MO Mohamed; MH Ahmed. *Turk J Chem*. **2006**, 30, 361-382.
[27] AMA Rawaa. Thesis, University of Baghdad, **2000**.
[28] JA Ahlam; MNK Asmaa. Proceeding of 3rd scientific conference of the college of science, University of Baghdad, **2009**, 1458-1471.
[29] WJ Geary. *Coordin Chem Rev*. **1971**, 17, 81-122.